Final Ti Model Results

Tigany Zarrouk

December 26, 2019

Contents

1 Objective Function

PARAMETERS fdd=0.1958363809 qdds=0.5591275855 qddp=0.5690351902 qddd=0.7745947522 b0=58.0906936439 p0=1.2185323579 b1=-3.2299188646 p1=0.6862915307 b2=593519.1134129359 m2=-11.5000000000 p2=0.0000000000 ndt=2.0000000000 cr1=-6.0000000000 cr2=3.0474400934 cr3=-1.2317472193 r1dd=6.5000000000 rcdd=10.0000000000 rmaxhm=10.1000000000 npar=18 VARGS -vfdd=0.1958363809 -vqdds=0.5591275855 -vqddp=0.5690351902 -vqddd=0.7745947522 -vb0=58.0906936439 -vp0=1.2185323579 -vb1=-3.2299188646 -vp1=0.6862915307 -vb2=593519.1134129359 -vm2=-11.5000000000 -vp2=0.0000000000 -vndt=2.0000000000 -vcr1=-6.0000000000 -vcr2=3.0474400934 -vcr3=-1.2317472193 -vr1dd=6.5000000000 -vrcdd=10.0000000000 -vrmaxhm=10.1000000000

Quantity	From Model	Target
a_{hcp}	5.58523112	5.57678969
c/a	1.58371266	1.58731122
a_{omega}	8.93475285	8.73254342
c_{omega}	5.38726911	5.32343103
a_{4h}	5.57584691	5.56325146
c_{4h}	18.09810672	17.75908031
a_{6h}	5.57365569	5.54639384
c_{6h}	27.18378460	26.77136353
a_{bcc}	6.20079768	6.17948863
a_{fcc}	7.87290654	7.88677000
DE(o,h)	0.58764167	-0.63343333
DE(4h,h)	1.58019500	3.17160000
DE(6h,h)	2.48264833	3.72005000
DE(b,h)	5.35128500	7.63520000
DE(f,h)	3.78088500	4.51880000
c_{11}	171.60928873	176.10000000
c_{33}	198.90063708	190.50000000
c_{44}	47.42549704	50.80000000
c_{12}	94.65941969	86.90000000
c_{13}	61.22624060	68.30000000
M_{freq0}	2.59341377	2.85858719
M_{freq1}	2.59341378	2.85858719
M_{freq2}	2.59341378	2.85858719
M_{freq3}	2.59341379	2.85858719
M_{freq4}	5.85272461	5.66706047
M_{freq5}	5.85272461	5.66706047
H_{freq0}	3.82320403	4.80643423
H_{freq1}	3.82320403	5.58010025
H_{freq2}	6.40288977	5.65316738
H_{freq3}	6.40288977	6.36651842
H_{freq4}	7.92857431	6.40050186
H_{freq5}	7.92857431	7.64082373
bandw. G	3.69394702	5.87085872
bandw. K	4.65178817	4.97424321
bandw. M	5.19329495	7.78109872
bandw. L	4.21232412	6.34433701
bandw. H	3.54700549	9.70902614
$DOSerr_h$	0.00000000	0.00000000
$DOSerr_o$	0.00000000	0.00000000
E_{prisf}	98.95340236	220.00000000

——— $E_{prismaticfault}$ ———

tbe:	98.953	mJ/m^2	
DFT:	250.000	mJ/m^2	[Benoit 2012]
DFT:	233.000	mJ/m^2	[Ackland 1999]

——— $E_{Basalfault}$ I2 ———

tbe:	211.658	mJ/m^2	
DFT:	260.000	mJ/m^2	[Benoit 2012]

2 Defect Clusters

——— $E_{vacancyformation}$ ———

tbe:	2.347 eV	
DFT:	1.950 eV	GGA-PAW: Angsten (2013)
exp:	1.270 eV	Hashimoto (1984)

2.1 Octahedral O interstitial relaxation

Initial:

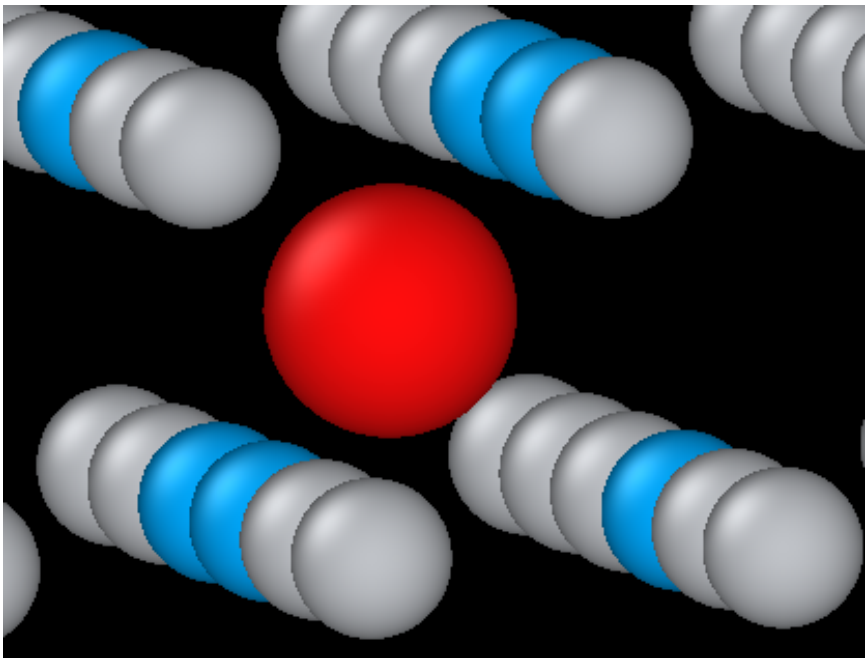

Final:

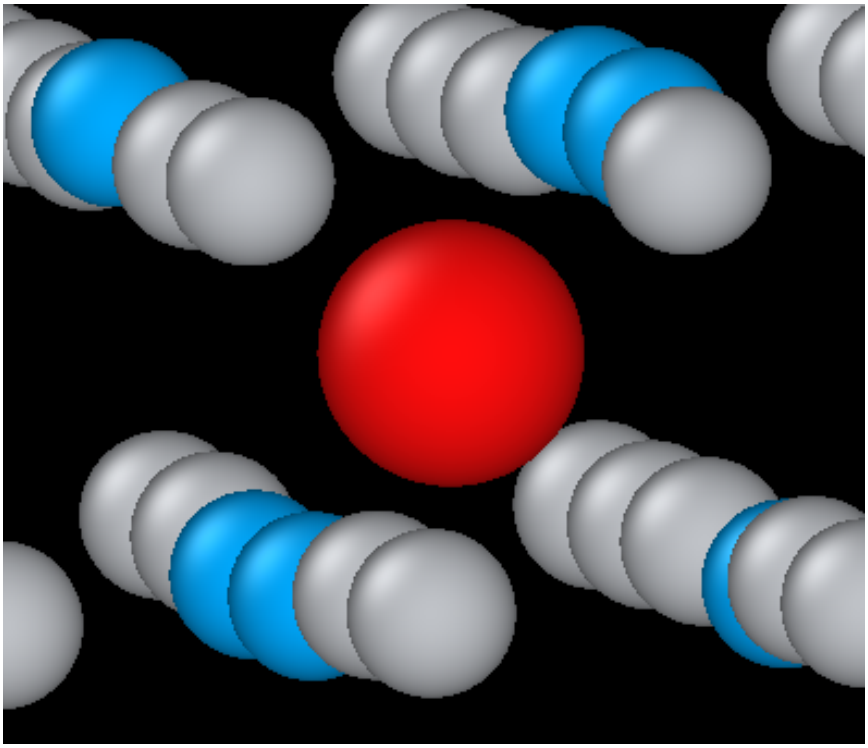

2.2 Tetrahedral O interstitial relaxation

Initial:

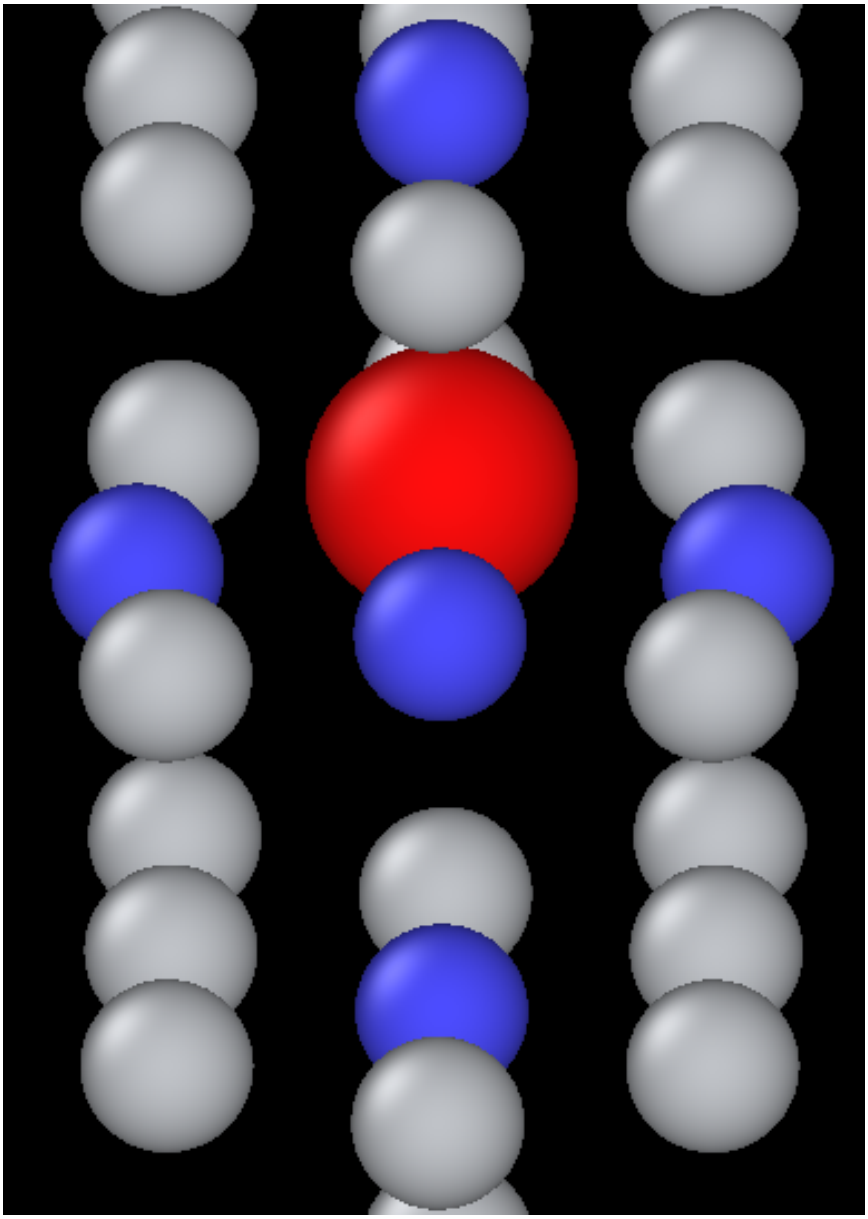

Final:

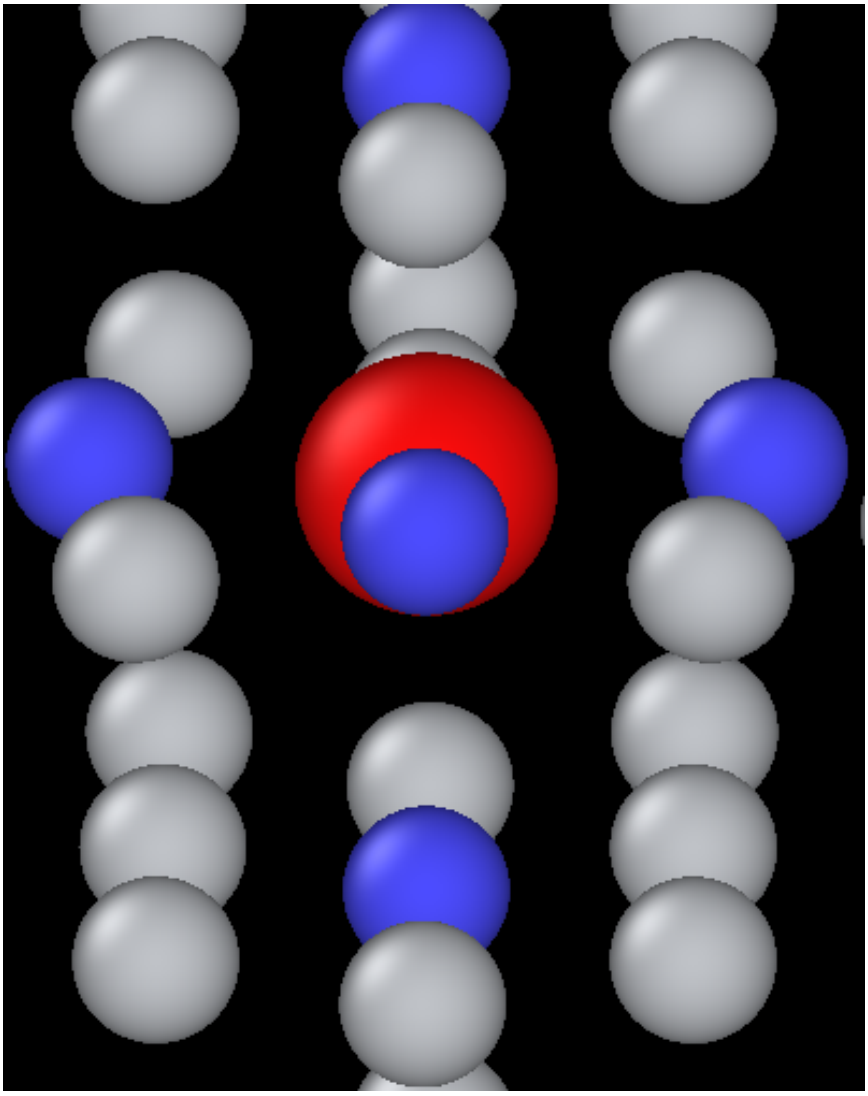

2.3 Energies for defects

Relative differences are

» ($E_{tetrahedral}$ - $E_{octahedral}$)

tbe:	1.65 eV	
GGA-DFT:	1.23 eV	Kwasniak (2013)

» ($E_{hexahedral}$ - $E_{octahedral}$)

tbe: 0.90 eV

> Note: Preference for tetrahedral oxygen to go into hexahedral site as seen by images above

All formation energies below use the chemical potential of Akysonov (2013) of value $\mu_{\text{oxygen}} = \frac{5.6}{2} eV$.

2.4 All formation energies

Quantity	Energy (eV)
Ef_{Vf}	2.347
Ef_{Tsol}	- 21.783
$Ef_{Tdilimp}$	- 28.991
$Ef_{Tformation}$	- 21.783
$Ef_{TVformation}$	- 18.905
$Ef_{Tvacsolbind}$	- 0.530
Ef_{Osol}	- 23.436
$Ef_{Odilimp}$	- 30.645
$Ef_{Oformation}$	- 23.436
$Ef_{OVformation}$	- 18.905
$Ef_{Ovacsolbind}$	- 2.183
Ef_{OOsol}	- 49.606
$Ef_{OOdilimp}$	- 56.814
$Ef_{OOformation}$	- 46.806
$Ef_{OOVformation}$	- 41.910
$Ef_{OOvacsolbind}$	- 2.547
Ef_{OOOsol}	- 76.037
$Ef_{OOOdilimp}$	- 83.246
$Ef_{OOOformation}$	- 70.437
$Ef_{OOOVformation}$	- 66.013
$Ef_{OOOvacsolbind}$	- 2.076
$Ef_{OOOOsol}$	- 102.470
$Ef_{OOOOdilimp}$	- 109.679
$Ef_{OOOOformation}$	- 94.070
$Ef_{OOOOVformation}$	- 88.998
$Ef_{OOOOvacsolbind}$	- 2.724
$Ef_{OOOOOsol}$	- 128.781
$Ef_{OOOOOdilimp}$	- 135.989
$Ef_{OOOOOformation}$	- 117.581
$Ef_{OOOOOVformation}$	- 113.649
$Ef_{OOOOOvacsolbind}$	- 1.583
$Ef_{OOOOOOsol}$	- 155.148
$Ef_{OOOOOOdilimp}$	- 162.357
$Ef_{OOOOOOformation}$	- 141.148
$Ef_{OOOOOOVformation}$	- 137.110
$Ef_{OOOOOOvacsolbind}$	- 1.690

3 Gamma surfaces

Energies are accurate to within 2 mJm^{-2}, comparing the energies of points in the corners which (the zeros of energy). So surface energies might be ± 2 mJm^{-2} off which is reasonable.

These calculations were done in tight binding with 15 layers for both basal and prismatic with k-points adjusted accordingly. DFT comparisons are usind results of Rodney.

The Pyramidal surface was obtained using the same 32 atom cell that Ready used in his paper on the pyramidal gamma surface with DFT pseudopotentials.

3.1 Basal

TBE:

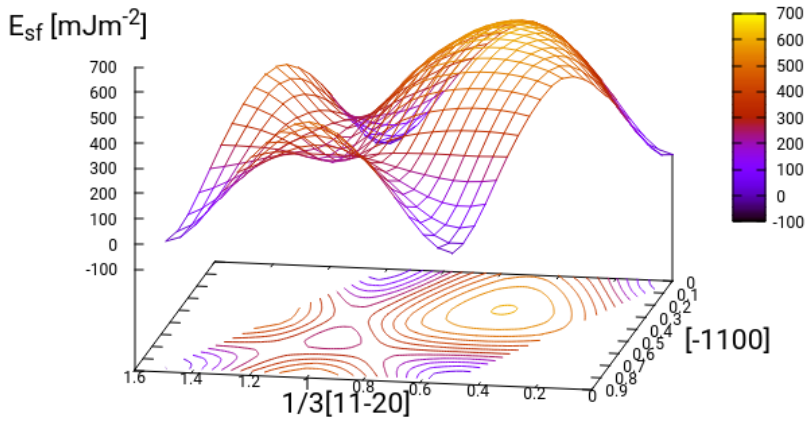

DFT:

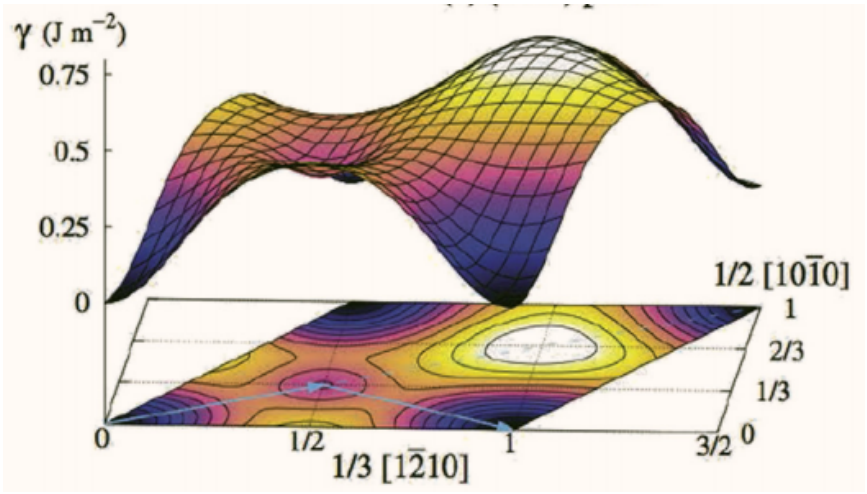

3.2 Prismatic

TBE:

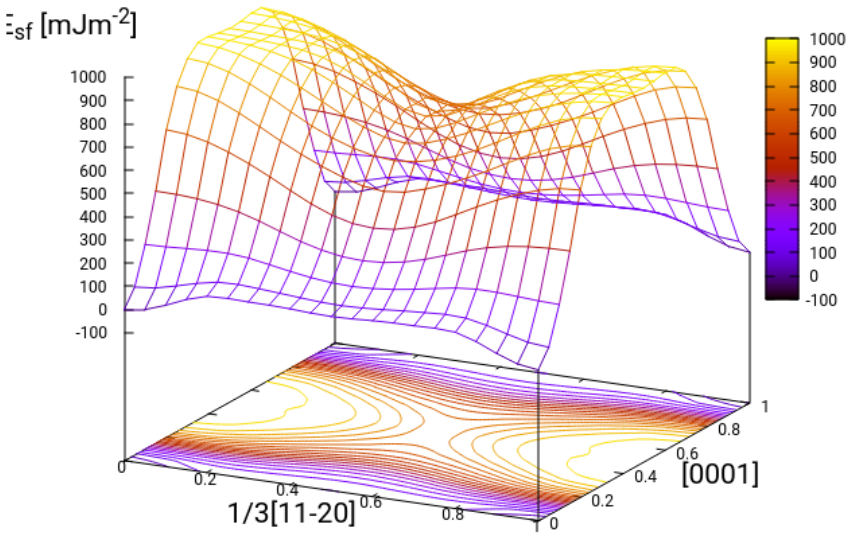
Esf [mJm-2]
1000
900
800
700
600
500
400
300
200
100
0
-100
1/3[11-20]
[0001]

DFT:

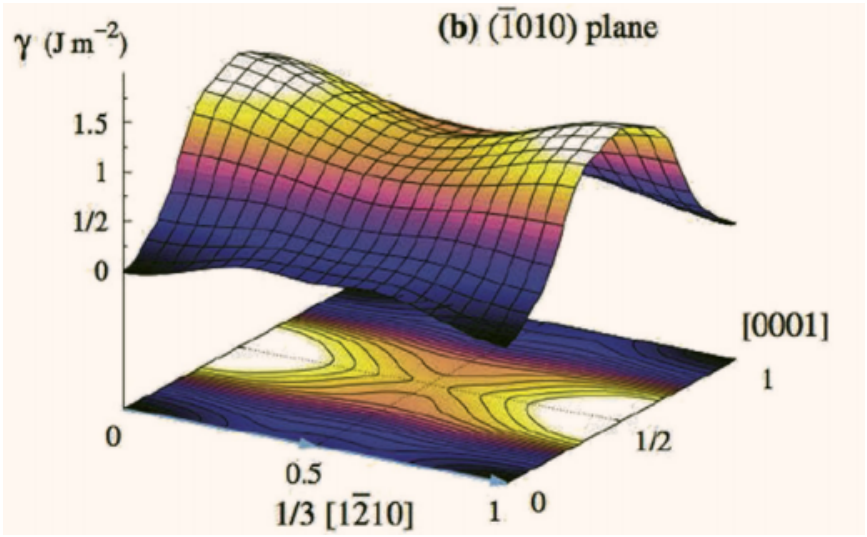
γ (J m−2)
(b) (1̄010) plane
1.5
1
1/2
0
[0001]
1
0.5
1/3 [12̄10]

3.3 Pyramidal first order

TBE:

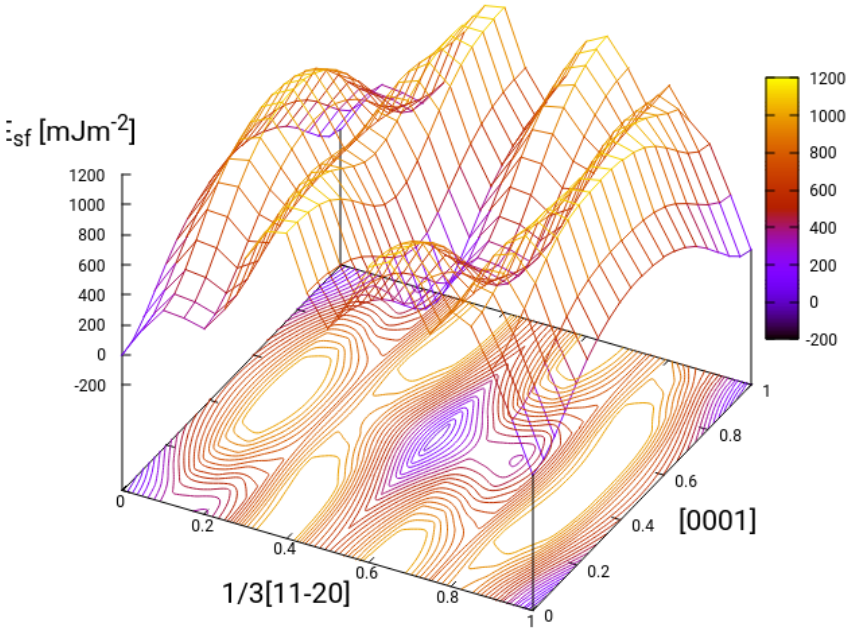

DFT pseudopot:

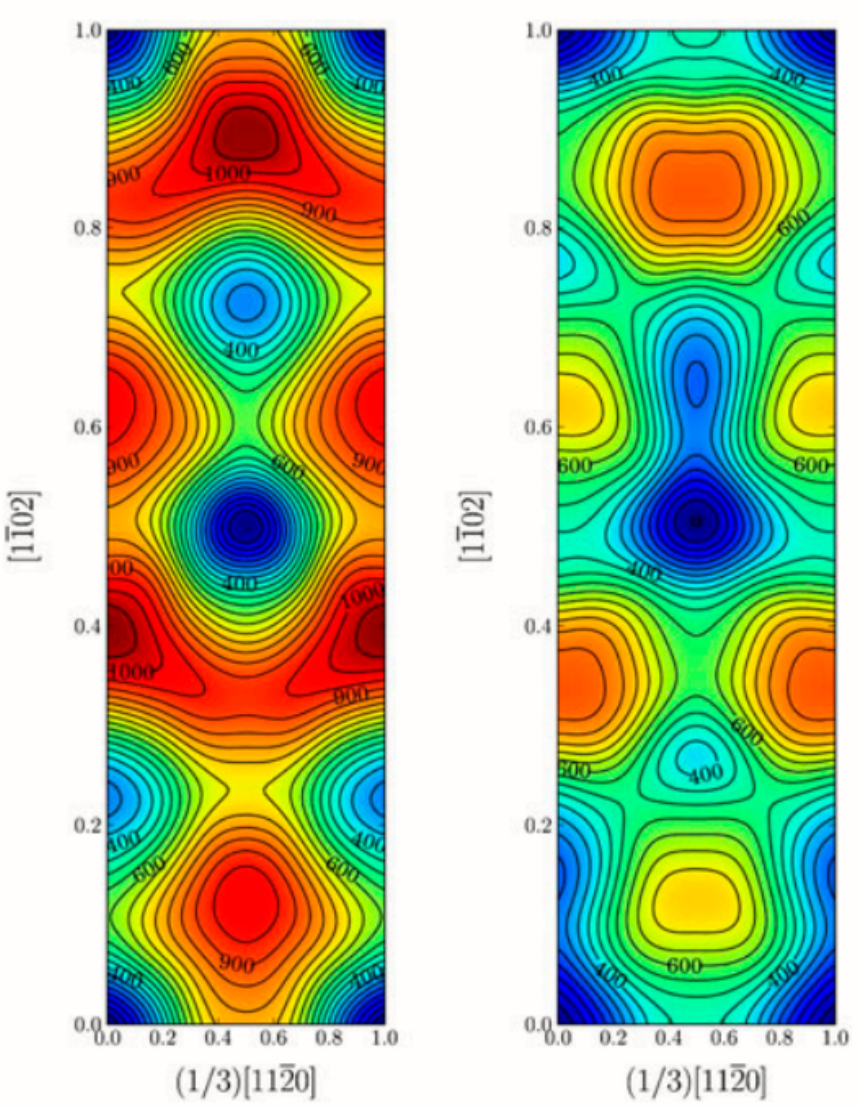

3.4 Data

$\text{basal}_{\text{gsdata}}$ $\text{prismatic}_{\text{gsdata}}$ $\text{pyramidal}_{\text{gsdata}}$

4 Dislocation core structures

In the following figures we have the partial differential displacement maps of dislocations in their initial and final state. The atoms were relaxed until

the root-mean square force acting on each atom was less than $1 \times 10^{-}5$ Ryd/Bohr.

These relaxations can be distinguished by the different initial positions of the dislocation centre (elastic centre) as following the paper by Tarrat [1].

The partial burger's vector seen here is the $1/6[11\bar{2}0]$ dislocation.

One can see that all of the dislocations have dissociated on the prismatic plane. But there is a difference between initial positions as to upon which prismatic plane they dissociate on, from the original.

Only initial position 2 actually dissociated on a different prismatic plane to the others.

There does seem to be a large dissociation distance.

There is a small energy difference between the dip in the prismatic gamma surface along the $1/3[11\bar{2}0]$ direction. This means that along that direction, due to the small relative energy barrier between the trough in the centre of the gamma surface line and the peaks, so to speak, the dislocation can dissociate easily along this direction.

The dissociation distance is consistent between the different initial positions of the elastic centres. The distance is $\approx 4c = 35.4$ Bohr $= 18.7$.

This is roughly double the distance that is found in the DFT Zr results by Clouet [2].

4.1 TODO Dissociation Distance Analysis

Following [2], one can dislocation elasticity theory to compute the dissociation distance of a dislocation in both the basal and prism planes. The energy variation caused by a dissociation length d is

$$\Delta E_{\text{diss}}(d) = -b_i^{(1)} K_{ij} b_j^{(2)} \ln\left(\frac{d}{r_c}\right) + \gamma d,$$

where $\mathbf{b}^{(i)}$ are the burger's vectors of the dissociated dislocations. γ is the corresponding gamma surface energy and K is the Stroh matrix. Controlling the dislocation core radius and the dislocation elastic energy, one can find the equilibrium dissociation distance as

$$d^{\text{eq}} = \frac{b_i^{(1)} K_{ij} b_j^{(2)}}{\gamma}$$

With the orientation of the simulation cell as, $U_1 = na\frac{1}{2}[10\bar{1}0]$, $U_2 = mc[0001]$, $U_3 = a\frac{1}{3}[1\bar{2}10]$, one finds the components of the Stroh matrix as:

$$K_{11} = \frac{1}{2\pi}\left(\bar{C}_{11} + C_{13}\right)\sqrt{\frac{C_{44}\left(\bar{C}_{11} - C_{13}\right)}{C_{33}\left(\bar{C}_{11} + C_{13} + 2C_{44}\right)}} \tag{1}$$

$$K_{22} = \sqrt{\frac{C_{33}}{C_{11}}}K_{11} \tag{2}$$

$$K_{33} = \frac{1}{2\pi}\sqrt{\frac{1}{2}C_{44}\left(C_{11} - C_{12}\right)} \tag{3}$$

here, $\bar{C}_{11} = \sqrt{C_{11}C_{33}}$.

From the gamma surface, for the basal plane one expects a dissociation of $1/3[1\bar{2}10] = 1/3[1\bar{1}00] + 1/3[0\bar{1}10]$. Then dissociation length in the basal plane is given by

$$d_{\mathrm{b}}^{\mathrm{eq}} = \frac{(3K_{33} - K_{11})a^2}{12\gamma_{\mathrm{b}}}$$

For the prism plane the $1/3[1\bar{2}10]$ dislocation can dissociate into $1/6[1\bar{2}10]\pm$ $\alpha(c/a)[0001]$ where the parameter α controls the position of the stacking fault minimum along the [0001] direction. Only in interatomic potentials like the EAM, do we find that $\alpha = 0.14$.

The dissociation length is

$$d_{\mathrm{p}}^{\mathrm{eq}} = \frac{(K_{33}a^2 - 4\alpha^2 K_{22}c^2)}{4\gamma_p}$$

4.2 TODO Disregistry Analysis

Look into the theory of dissociation distance in Clouet paper [2]

Disregistry given by the Peierls-Nabarro model. Analytic expression given in Hirth and Lothe [3].

Disregistry $D(x)$ is defined as the displacement difference between the atoms in the plane just above and those just below the dislocation glide plane. The derivative of this function $\rho(x) = \partial D/\partial x$ corresponds to the dislocation density.

$$D_{\mathrm{dislo}} = \frac{b}{2\pi}\left\{\arctan\left[\frac{x - x_0 - d/2}{\zeta}\right] + \arctan\left[\frac{x - x_0 + d/2}{\zeta} + \frac{\pi}{2}\right]\right\}$$

Given x_0 is the dislocation position, d is dissociation length and ζ is the spreading of each partial dislocation.

$$
\begin{aligned}
D_L = & \sum_{n=-\infty}^{\infty} D_{\text{dislo}}(x - nL) \\
= & \frac{b}{2\pi}\Bigg\{ \arctan\left[\frac{\tan\left(\frac{\pi}{L}[x - x_0 - d/2]\right)}{\tanh\left(\frac{\pi\zeta}{L}\right)}\right] + \pi\left\lfloor \frac{x - x_0 - d/2}{\zeta} + \frac{1}{2}\right\rfloor \\
& + \arctan\left[\frac{\tan\left(\frac{\pi}{L}[x - x_0 + d/2]\right)}{\tanh\left(\frac{\pi\zeta}{L}\right)}\right] + \pi\left\lfloor \frac{x - x_0 + d/2}{\zeta} + \frac{1}{2}\right\rfloor\Bigg\},
\end{aligned}
$$

where $\lfloor\cdot\rfloor$ is the floor function.

For an array of dislocations in the S arrangement, $D(x) = D_L(x)$, with $L = mc$, where m is the number of repeated unit cells in the U_2 direction.

Here, $U_1 = na\frac{1}{2}[10\bar{1}0]$, $U_2 = mc[0001]$, $U_3 = a\frac{1}{3}[1\bar{2}10]$.

This procedure therefore allows us to determine the location of the dislocation center. For all interaction models, we find that this center lies in between two (0001) atomic planes. One can see in Fig. 6 of [2] that this position corresponds to a local symmetry axis of the differential displacement map. This is different from the result obtained by Ghazisaeidi and Trinkle [4] in Ti where the center of the screw dislocation was found to lie exactly in one (0001) atomic plane.

4.3 IP1

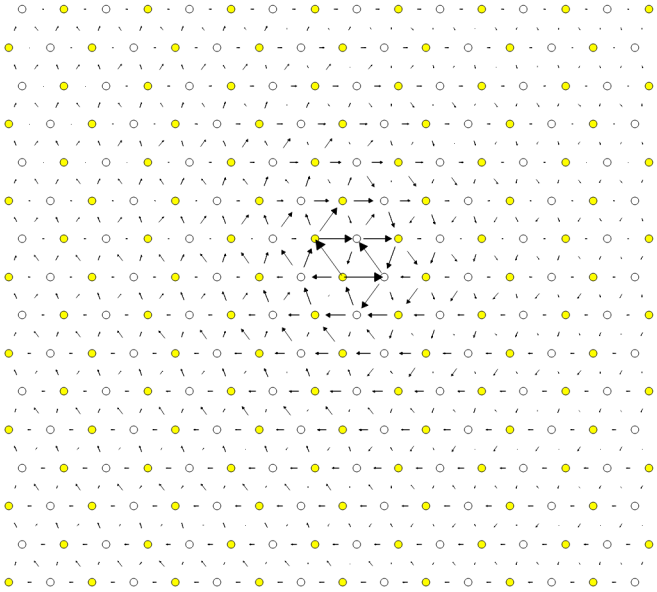

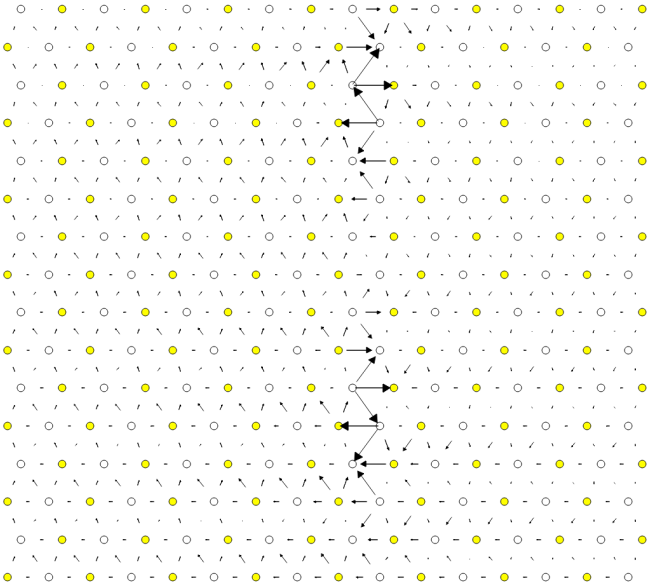

4.4 IP2

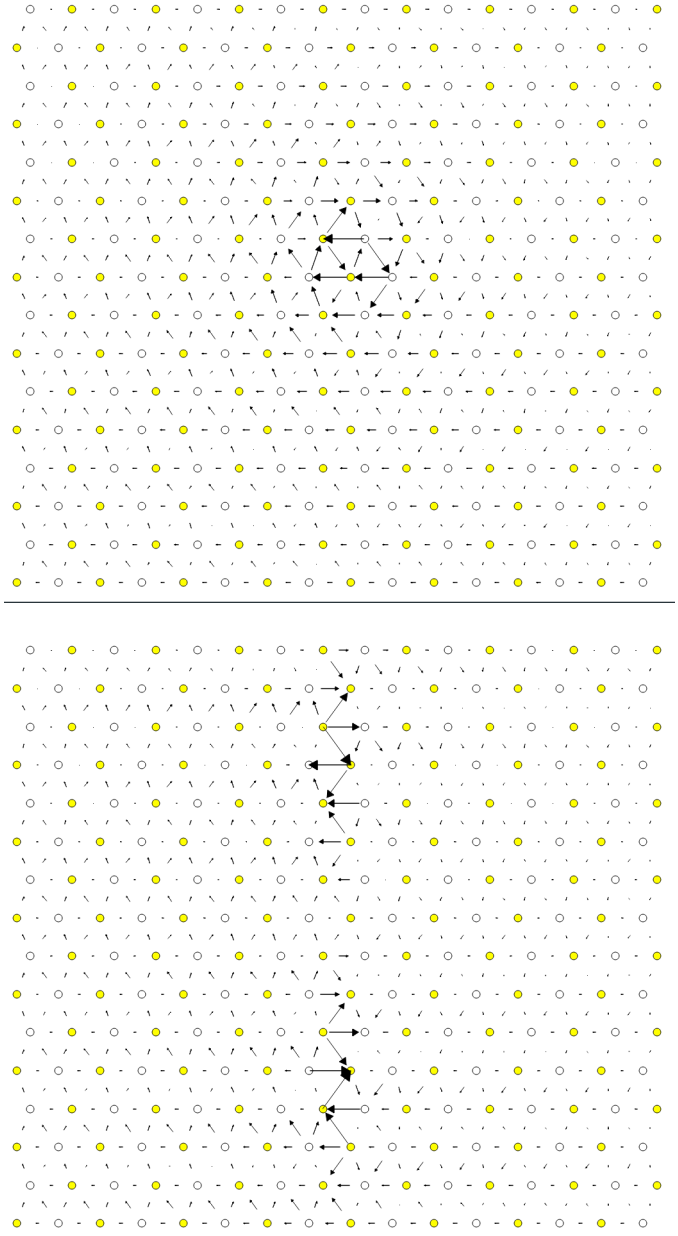

4.5 IP3

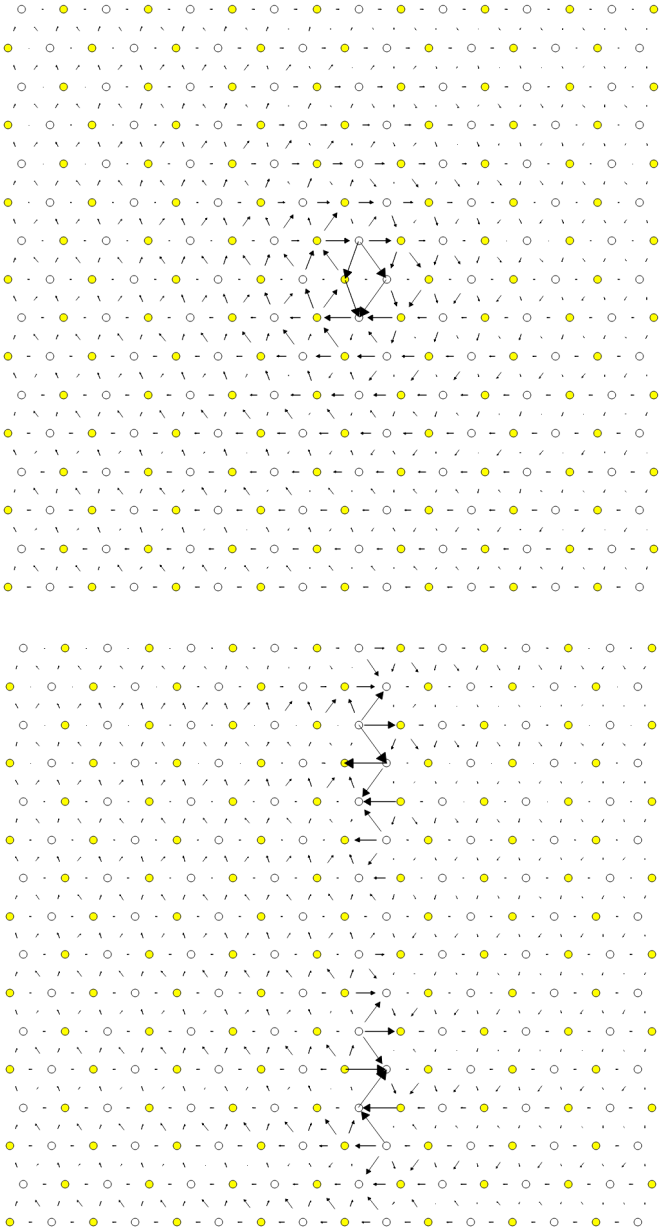

4.6 IP4

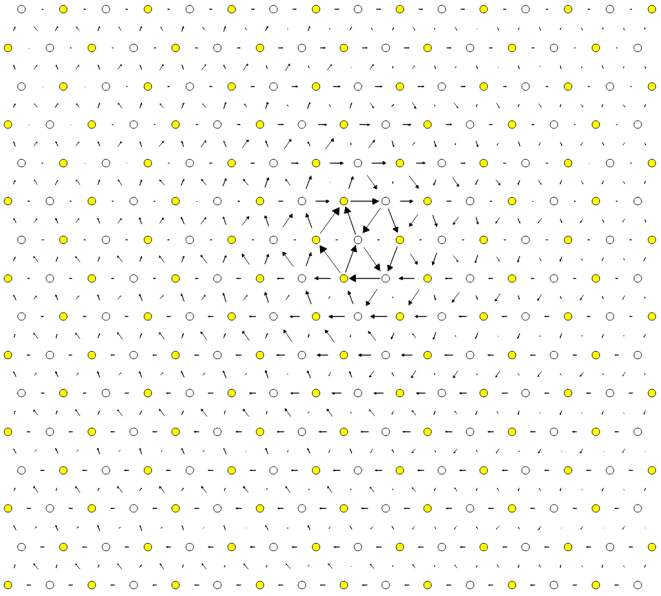

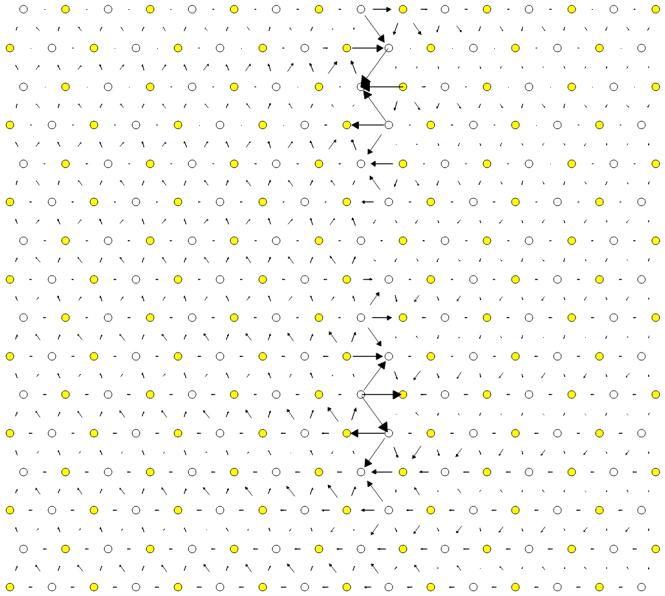

4.7 IP5

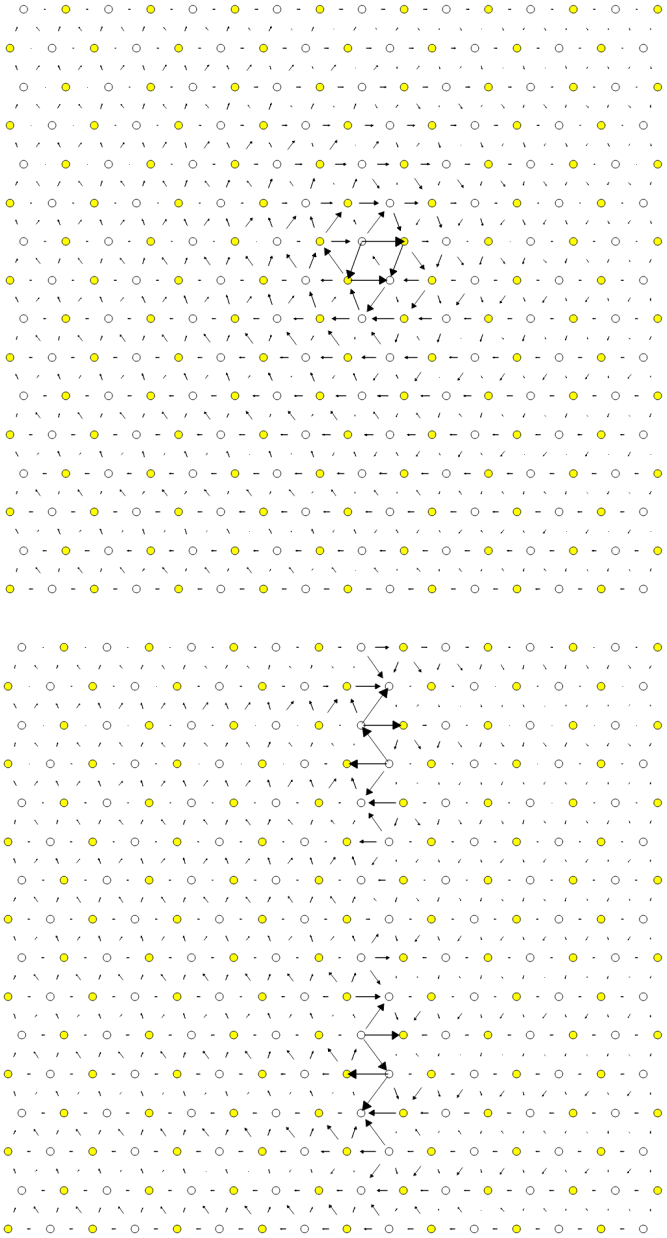

4.8 Ghazisaeidi Results for comparison

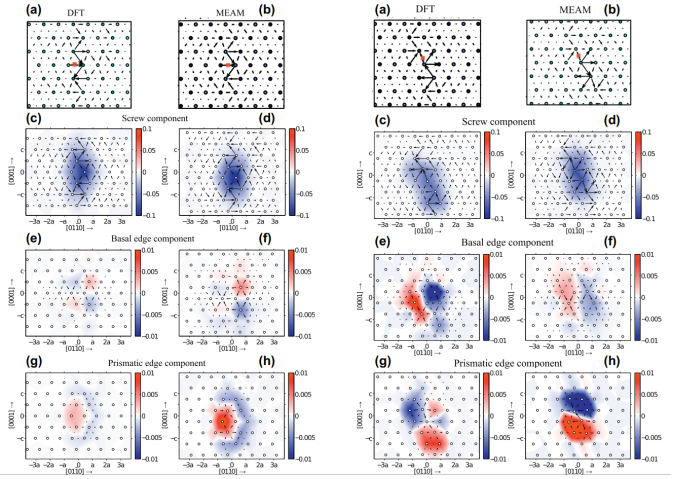

4.9 Peierls Stress

By straining lattice and incrementally increasing the strain, one can find the minimum stress necessary to move a dislocation from one Peierls valley to the next.

4.9.1 xy strain 0.03

Here the α parameter is 0.03.

This means that the stress necessary to move the dislocation is

$$\begin{aligned}\sigma_{12} &= C_{1212}\varepsilon_{12} \\ &= 2C_{66}^{\text{Voigt}}\varepsilon_{6}^{\text{Voigt}} \\ &= (C_{11} - C_{12})\varepsilon_{6}^{\text{Voigt}} \\ &= 76.59 \times 0.03 \\ &= 2.31GPa\end{aligned}$$

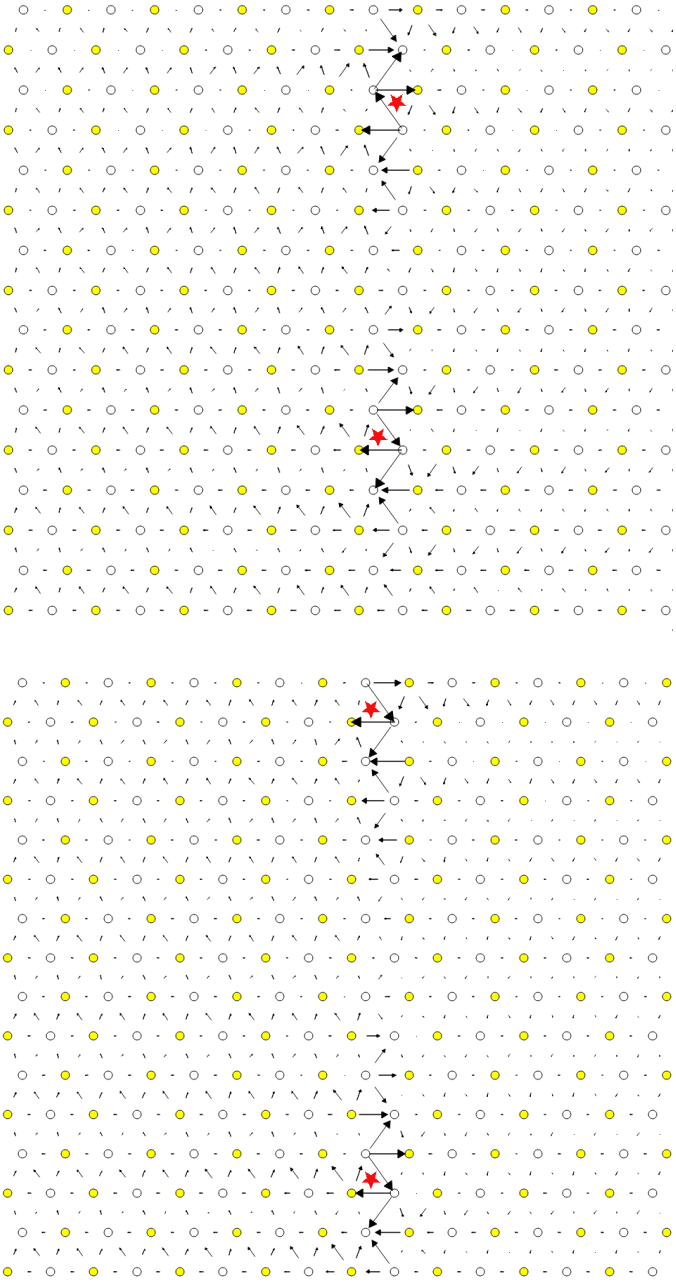

4.10 Data

IP1 IP2 IP3 IP4 IP5

4.11 Directory of the results

`file:///home/tigany/Documents/ti/2019-09-11_final_model/tbe/dislocations/2019-11-08_no_omega_ordering_ec_latpar/` `file:///home/tigany/Documents/ti/final_model_2019-11`

5 BOP

5.1 4 recursion levels

kbT = 0.1

» Lattice parameters:

> hcp

a	2.901660 Å
c	4.747485 Å
etot	-18.342162 eV

> omega

a	7.917318 Å
c	2.749892 Å
etot	-17.458700 eV

Omega is still not as stable as hcp as expected from model.

» Elastic Constants

Quantity	calc. (10^{11} Pa)	exp. (10^{11} GPa)
C11	1.781	1.761
C12	0.738	0.868
C13	0.611	0.682
C33	1.969	1.905
C44	0.285	0.508
C66	0.522	0.450
K	1.050	1.101
R	0.669	0.618
H	0.558	0.489

6 Bibliography

References

[1] Nathalie Tarrat, Magali Benoit, and Joseph Morillo. Core structure of screw dislocations in hcp ti: an ab initio DFT study. *International Journal of Materials Research*, 100(3):329–332, mar 2009.

[2] Emmanuel Clouet. Screw dislocation in zirconium: An ab initio study. *Physical Review B - Condensed Matter and Materials Physics*, 86(14):1–11, 2012.

[3] P.M. Anderson, J.P. Hirth, and J. Lothe. *Theory of Dislocations*. Cambridge University Press, 2017.

[4] M. Ghazisaeidi and D.R. Trinkle. Core structure of a screw dislocation in ti from density functional theory and classical potentials. *Acta Materialia*, 60(3):1287–1292, feb 2012.